Environmental Research Letters

LETTER

Long term trend and interannual variability of land carbon uptake–the attribution and processes

Zheng Fu[1,2,3], Jinwei Dong[4], Yuke Zhou[1], Paul C Stoy[3] and Shuli Niu[1,2,5]

[1] Key Laboratory of Ecosystem Network Observation and Modeling, Institute of Geographic Sciences and Natural Resources Research, CAS, Beijing 100101, People's Republic of China
[2] University of Chinese Academy of Sciences, No.19A Yuquan Road, Beijing, 100049, People's Republic of China
[3] Department of Land Resources and Environmental Sciences, Montana State University, Bozeman, MT 59717, United States
[4] Key Laboratory of Land Surface Pattern and Simulation, Institute of Geographic Sciences and Natural Resources Research, CAS, Beijing 100101, People's Republic of China
[5] Author to whom any correspondence should be addressed.

E-mail: sniu@igsnrr.ac.cn

Keywords: long term trend of carbon uptake, interannual variability of carbon uptake, carbon uptake amplitude, carbon uptake duration, Northern Hemisphere, Southern Hemisphere

Supplementary material for this article is available online

OPEN ACCESS

RECEIVED
14 June 2016

REVISED
23 December 2016

ACCEPTED FOR PUBLICATION
4 January 2017

PUBLISHED
23 January 2017

Abstract

Ecosystem carbon (C) uptake in terrestrial ecosystems has increased over the past five decades, but with large interannual variability (IAV). However, we are not clear on the attribution and the processes that control the long-term trend and IAV of land C uptake. Using atmospheric inversion net ecosystem exchange (NEE) data, we quantified the trend and IAV of NEE across the globe, the Northern Hemisphere (NH), and the Southern Hemisphere (SH), and decomposed NEE into carbon uptake amplitude and duration during each year from 1979–2013. We found the NH rather than the SH determined the IAV, while both hemispheres contributed equivalently to the global NEE trend. Different ecosystems in the NH and SH had differential relative contributions to their trend and IAV. The long-term trends of increased C uptake across the globe and the SH were attributed to both extended duration and increasing amplitude of C uptake. The shortened duration of uptake in the NH partly offsets the effects of increased NEE amplitude, making the net C uptake trend the same as that of the SH. The change in NEE IAV was also linked to changes in the amplitude and duration of uptake, but they worked in different ways in the NH, SH and globe. The fundamental attributions of amplitude and duration of C uptake revealed in this study are helpful to better understand the mechanisms underlying the trend and IAV of land C uptake. Our findings also suggest the critical roles of grassland and croplands in the NH in contributing to the trend and IAV of land C uptake.

Introduction

Since the 1960s, the land has acted as a substantial sink for atmospheric carbon dioxide (CO_2), sequestering about one-quarter of fossil-fuel emissions during an average year (Ballantyne *et al* 2012). The magnitude of land carbon (C) sink has increased over the past decades (Keenan *et al* 2016) but varies largely from year to year (Quéré *et al* 2013). The patterns have been well recognized, but the attribution and processes for causing the long-term trend and interannual variability (IAV) of land C uptake (net ecosystem exchange in a given year) remain far from clear.

The northern hemisphere (NH) and southern hemisphere (SH) differ in the dynamics of ecosystem C uptake (Field *et al* 1998, Schimel *et al* 2001), which may contribute differentially to the trend and IAV of land C sinks. In the NH, observational evidence has shown the increasing land C uptake and enhancement of terrestrial vegetation growth over the past decades (Forkel *et al* 2016, Nemani *et al* 2003, Tucker *et al* 2001, Zhou *et al* 2001). This long-term increase of land C uptake in the NH was attributed to different factors, including the increased CO_2 concentrations (Ahlbeck 2002, Kohlmaier *et al* 1989, Myneni *et al* 1997), climate warming (DeRosier *et al* 1996, Piao *et al* 2006),

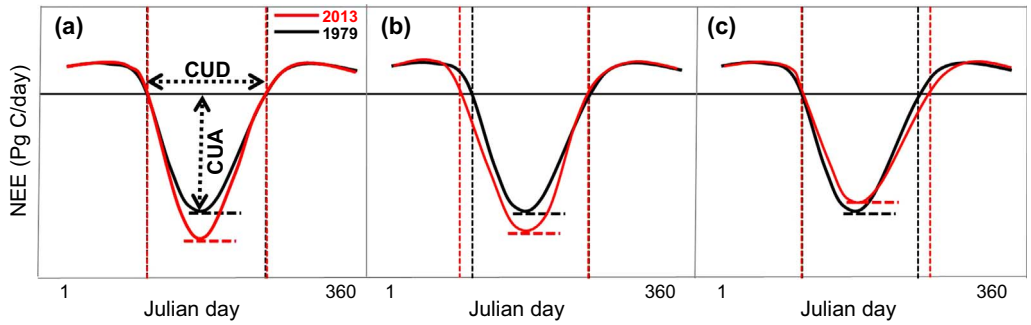

Figure 1. Conceptual figure of carbon uptake amplitude (CUA) and carbon uptake duration (CUD) in determining the changes in annual ecosystem C uptake from 1979 to 2013. (*a*) An increase in CUA without a change in CUD. (*b*) An increase in CUA with simultaneous increase in the starting date of carbon uptake. (*c*) A decline in CUA and changing end date of carbon uptake. This conceptual figure only shows partly the representative scenarios rather than all the possible combinations and hypotheses, including scenarios where the CUD is invariant.

precipitation (Piao *et al* 2006), nitrogen deposition (Pan *et al* 2009), afforestation (Fang *et al* 2001), longer growing seasons (DeRosier *et al* 1996), expanded distribution of trees and shrubs (Forkel *et al* 2016, Pan *et al* 2011), and agriculture following the 'green revolution' (Gray *et al* 2014, Zeng *et al* 2014). However, in the SH, the land C uptake exhibits large year-to-year variability with uncertain long term trends. Tropical forest deforestation has increased widely (Pan *et al* 2011) and tropical lands have experienced increasing drought and heat in the SH over the past decades (Allen *et al* 2010, Phillips *et al* 2009, Zhao and Running 2010), which might reduce the land C sink in the SH. But the large areas of semi-arid ecosystems with dryness-controlled in the SH (Yi *et al* 2010, Yi *et al* 2014), responded quickly to precipitation events and led to a large amount of C uptake (Ma *et al* 2016), which was assumed to contribute largely to the IAV of land C uptake (Ahlström *et al* 2015, Frank *et al* 2015, Ma *et al* 2016, Poulter *et al* 2014). Meanwhile, widespread observations and satellite remote sensing showed that vegetation expanded with woody encroachment over semi-arid areas and increased vegetation greenness over recent decades (Andela *et al* 2013, Donohue *et al* 2009, Fensholt *et al* 2012), which increased the SH land C sink. Thus, the NH and SH may play different roles in the trend and IAV of land C uptake. A comprehensive analysis of the relative contributions of the NH and SH to the trend and IAV of land C uptake has so far been lacking.

Different ecosystem types may also play various roles in regulating the changes in land C uptake. At the global scale, Ahlström *et al* (2015) found recently that semi-arid ecosystems contributed approximately 39% of the IAV in net biome production, while tropical ecosystems, extra-tropical forests, grasslands and croplands contributed 19%, 11% and 27%, respectively. Since ecosystems are distributed quite differently in the NH (largely comprising grasslands and croplands, tundra and arctic shrub lands, extra-tropical forests) and the SH (largely comprising semi-arid and tropical forests), we need to quantify the specific contributions of different ecosystems to the trend and IAV in the NH and SH in order to better understand the attribution regions.

For a process-based understanding, changes in annual C uptake can be decomposed into carbon uptake duration (CUD) and carbon uptake amplitude (CUA) (Gu *et al* 2009, Xia *et al* 2015). As the concept figure (figure 1) shows, numerous hypotheses can be proposed for the regulation of CUA and CUD on the changes in annual land C uptake. Increasing CUA without changes in CUD (figure 1(*a*)) will enhance land C uptake. Increasing CUA and simultaneously changing CUD by advancing the starting date of C uptake (figure 1(*b*)) could also increase the C uptake. Decreasing CUA but lengthening CUD by postponing the ending date of C uptake (figure 1(*c*)) may change the amount of annual ecosystem C uptake as well. However, we have limited understanding on how CUA and CUD regulate observed trends and IAV of land C uptake.

The purpose of this study was to quantify the relative contributions of different ecosystems in the NH and SH and to understand the key processes of CUA and CUD in controlling the trend and IAV of global land C uptake. Specifically, this study was conducted to address (1) how the NH and SH contribute to the trend and IAV in the land C sink over recent decades; (2) how different ecosystems in the NH and SH contribute to their trend and IAV, (3) how CUA and CUD differentially determine the trend and IAV of land C uptake in NH, SH and globe.

Methods

Atmospheric inversion data

Atmospheric inversion data used in this study were based on the Monitoring Atmospheric Composition and Climate (MACC- III) inversion system version 13.1 (http://apps.ecmwf.int/datasets/data/macc-ghg-inversions/). The dataset describes the CO_2 surface fluxes during the period 1979–2013 with a resolution of 3.75 ° × 1.875 ° (longitude-latitude) and a 3-hourly

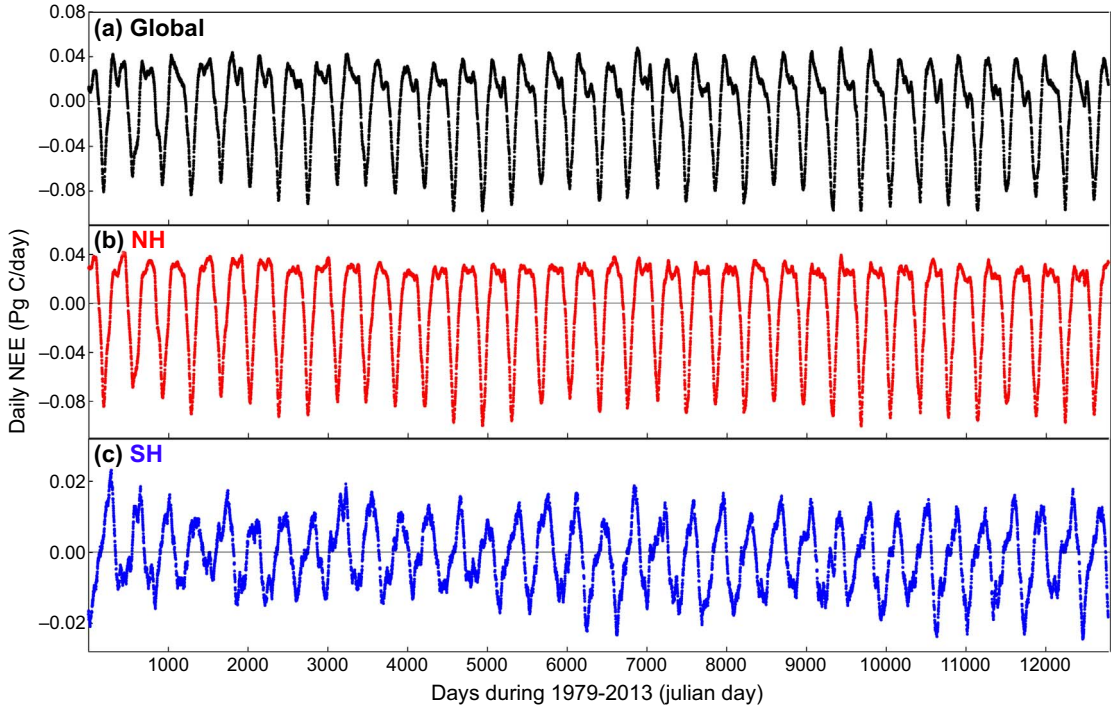

Figure 2. The daily net ecosystem exchange (NEE) calculated from atmospheric inversion data during 1979–2013 in the globe (*a*), Northern Hemisphere (NH, (*b*)) and Southern Hemisphere (SH, *c*).

time step using atmospheric CO_2 data sets from a global network (NOAA/ESRL,WDCGG, CarboEurope and RAMCES) of continuous and discrete flask samples (Chevallier *et al* 2007, Chevallier *et al* 2010). Fluxes and mole fractions are linked in the system by a global atmospheric transport model. The flux inversion builds on a variational Bayesian inversion system, like the 4D-Var data assimilation system used in MACC-II, which allows the fluxes to be estimated at relatively high resolution over the globe (Chevallier *et al* 2007, Chevallier *et al* 2010, Chevallier *et al* 2005). A robust Monte Carlo method from the Bayesian theory was used to quantify the uncertainty of the inverted fluxes (Chevallier *et al* 2007, Chevallier *et al* 2010, Chevallier *et al* 2005).

Definitions and calculations for CUD and CUA

We calculated the daily net ecosystem exchange (NEE) across the globe, NH and SH, which showed clearly seasonal dynamics during the 1979–2013 study period (figure 2). The sign convention of NEE is from the perspective of the atmosphere such that NEE is negative for ecosystem C uptake, and positive for release to the atmosphere. The starting date of C uptake was quantified as the date when the ecosystem switched from a CO_2 source to a sink, while ending date of C uptake was the date when the ecosystem switched from a CO_2 sink to a source. We defined the carbon uptake duration (CUD) as the number of days between the CO_2 sink starting date and ending date (figure 1(*a*)). The CUA is defined as the maximum value of daily land C sink that was derived from the peak of NEE seasonal dynamics (figure 1(*a*)). Considering that magnitude of C source changes also change the annual net C uptake, we defined the maximum value of daily C source as carbon release amplitude (CRA). We calculated the CUA, CRA, CUD, and starting and ending dates of land C uptake during each year from 1979 to 2013.

Calculation of trend and IAV and statistical analysis

We calculated the annual NEE across the globe, NH, and SH during each year from 1979 to 2013. The normality of the dataset was assessed using the Shapiro-Wilk method, which showed that all datasets followed a normal distribution (table S1). Simple linear regression was used to detect trends in NEE, CUA, CRA, CUD, starting date and ending date of ecosystem C uptake in the NH, SH, and globe with time. The statistical significance of the trend was also analyzed using the Mann-Kendall trend test (table S2). A *P* value of 0.05 was used to indicate a statistically significant trend. The anomalies of NEE, CUA, CUD, starting and ending data of C uptake in each year were detrended by subtracting the linear regression value from the original value (Ahlström *et al* 2015, Wang *et al* 2014).

We calculated the relative contributions of the NH and SH to the trend and IAV of global NEE, and further partitioned the trend and IAV of NEE in the NH and SH to different land cover classes according to their relative contributions. We divided the global land area into six land cover classes as in Ahlström *et al* (2015) using the MODIS MCD12C1 land cover classification (Friedl *et al* 2010), which includes extra-tropical forest, tropical forests, grasslands and croplands, semi-arid ecosystems, tundra and arctic

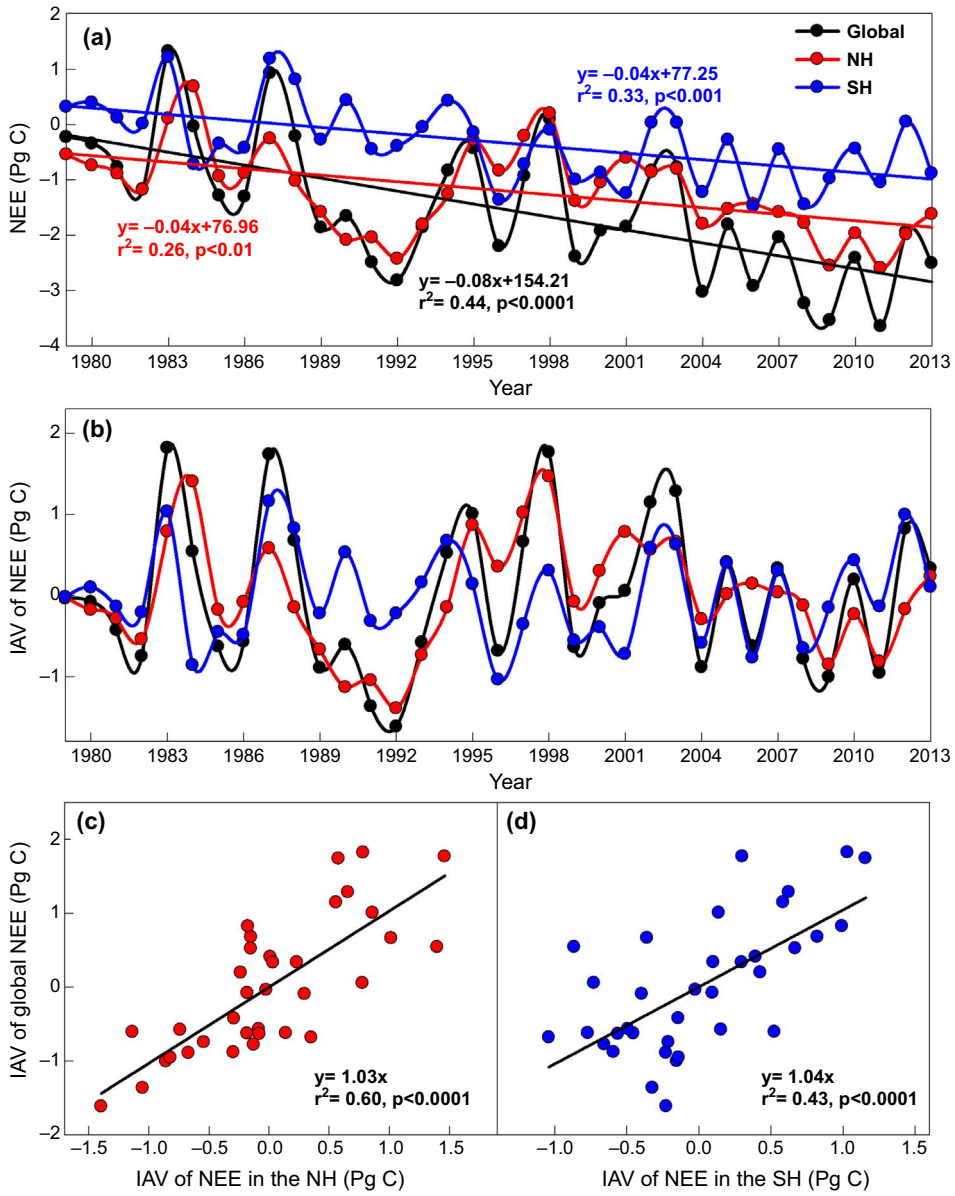

Figure 3. The long term trend (*a*) and interannual variability (IAV, (*b*)) of land C uptake across the globe, the northern hemisphere (NH), and the southern hemisphere (SH) during 1979–2013. The relationship between the IAV of the global land C uptake and the IAV of C uptake in the NH (*c*) and SH (*d*).

shrub lands, and sparsely vegetated lands (figure S1). Using the same methods of quantifying relative contributions as in Ahlström *et al* (2015), we adopted an index that scores individual geographic locations according to the consistency, over time, with which the local NEE flux resembles the sign and magnitude of the NH/SH NEE:

$$f_i = \frac{\sum_t \frac{x_{it}|X_t|}{X_t}}{\sum_t |X_t|}$$

where x_{it} is the NEE anomaly for region i at time t (in years), and X_t is the NH/SH NEE anomaly, such that $X_t = \sum_i x_{it}$. By this definition, f_i is the average relative NEE anomaly x_{it}/X_t for region i, weighted with the absolute NH/SH NEE anomaly $|X_t|$. The resulting scores for a region (f_i) represent its contribution to the NH/SH variations.

The relationships of CUA and CUD with the long-term trend of NEE, and the relationships of yearly CUA and CUD anomalies with IAV of NEE in the globe, NH, and SH, were tested using regression analysis and were considered significant with $P < 0.05$. Statistical analyses were conducted with SigmaPlot 12.5 for Windows.

Results

Trend and IAV of land C uptake across the globe, NH, and SH

In general, the land C sink (NEE for a given year) in the NH and SH both increased by 0.04 Pg C yr^{-1} ($P < 0.01$) over the past 35 years, resulting in an increase in the global land C sink of 0.08 Pg C yr^{-1} ($P < 0.0001$) (figure 3(*a*)). Although the land C sink across the globe, NH, and SH increased over the past

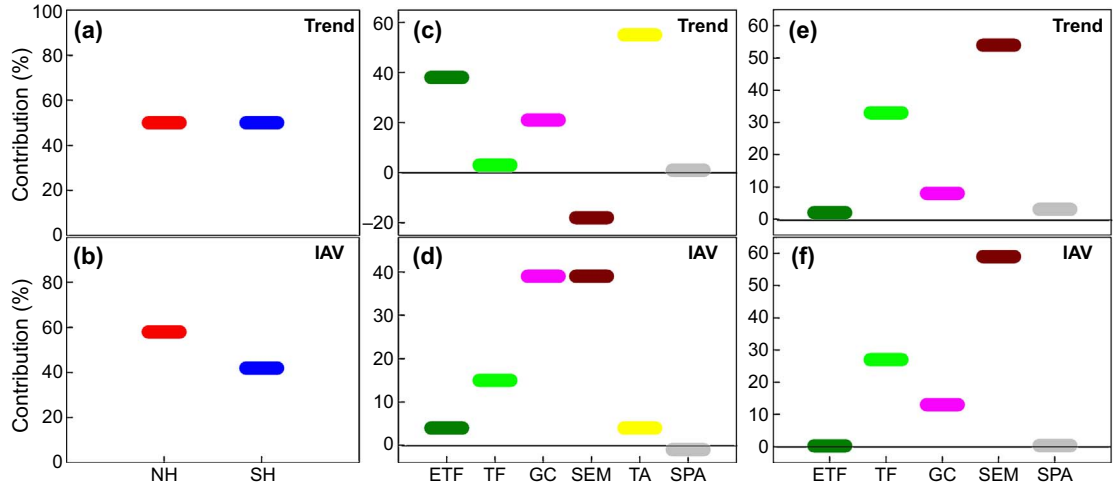

Figure 4. Contribution of the NH (*a*) and SH (*b*) to the trend and IAV of global NEE, and contribution of different land cover classes to the trend and IAV in the NH (*c*), (*d*) and SH (*e*), (*f*) (1979–2013). ETF: extra-tropical forest, TF: tropical forests, GC: grasslands and croplands, SEM: semi-arid ecosystems, TA: tundra and arctic shrub lands, SPA: sparsely vegetated lands. See the figure 3 for abbreviations.

35 years, they released CO_2 in 1983 (figure 3(*a*)). The mean land C uptake across the 35 year study period across the globe (1.52 Pg C yr^{-1}) and NH (1.19 Pg C yr^{-1}) were far more than that of SH (0.33 Pg C yr^{-1}).

IAV of global land C uptake showed strong agreement with those of NH and SH (figure 3(*b*)). The IAV of NH and SH C uptake was significantly correlated with the IAV of global NEE (all $P < 0.0001$), with a stronger correlation observed in the NH (figures 3(*c*) and (*d*)).

Relative contributions of different ecosystems in the NH and SH

The NH and SH both accounted for 50% of the trend of the global land C sink (figure 4(*a*)), but the relative contribution of the NH and the SH to the IAV of global land C sink were 58% and 42%, respectively (figure 4(*b*)).

Different land cover classes had various contributions to the trend and IAV of C uptake in the NH and SH. In the NH, tundra and arctic shrub lands (55%), extra-tropical forests (38%), and grasslands and croplands (21%) accounted for the largest fraction of the trend of C sink over this period, while semi-arid ecosystems (−18%) had negative contributions (figure 4(*c*)). In the SH, the trend of C sink was mostly contributed by semi-arid ecosystems (54%) and tropical forests (33%) (figure 4(*e*)). For the IAV of land C sink in the NH, we found that grasslands and croplands (39%) and semi-arid ecosystems (39%) were the dominant contributing regions (figure 4(*d*)). The dominant contribution regions to SH NEE IAV were semi-arid ecosystems (59%) and tropical forests (27%), as well as grasslands and croplands (13%, figure 4(*f*)).

The attribution process of CUA and CUD to the trend of C uptake

Across the 35 years, land C uptake significantly correlated with the carbon uptake amplitude (CUA) ($r^2 = 0.56, 0.41, 0.43$, all $P < 0.0001$) and carbon uptake duration (CUD) ($r^2 = 0.27, 0.31, 0.48$, for the globe, NH and SH, respectively, all $P < 0.01$) (figure S2). Although mean CUA across the globe and NH was significantly larger than that of the SH over the 35 years, CUA across the globe, NH and SH all increased by 0.0004, 0.0003 and 0.0002 Pg C d^{-1} yr^{-1}, respectively (figure 5(*a*)). CUD in the NH significantly decreased by 0.31 d yr^{-1} (figure 5(*b*)), while CUD in the SH and the globe did not significantly change over the past 35 years. However, if we removed the extreme high values observed in 1981, CUD across the globe also significantly increased by 0.41 d yr^{-1} (figure 5(*b*)). Note that each hemisphere's CUD is not linearly related to global changes in CUD as the two hemispheres are out of phase.

The change of CUD was determined by the start and end date of land C uptake. At the global scale, both the starting and ending date of C uptake significantly advanced by 0.64 and 0.36 d yr^{-1}, respectively (figure 5(*c*)), extending the CUD by 0.28 d yr^{-1} across the 35 years (figure 5(*c*)). The starting and ending dates of C uptake in the NH were significantly advanced by 0.21 and 0.52 d yr^{-1}, respectively, (figure 5(*d*)), reducing the CUD by 0.31 d yr^{-1} (figures 5(*b*) and (*d*)). Decreased CUD in the NH weakened the impacts of CUA increase on annual C uptake. In the SH, however, the starting date of C uptake advanced by 0.09 d yr^{-1} while the end date postponed 0.17 d yr^{-1} (figure 5(*e*)), extending the CUD by 0.26 d yr^{-1} across the 35 years (figure 5(*e*)). Extended CUD and increased CUA led to significant increase in NEE in the SH over the past 35 years (figure 3(*a*)). Overall, the trend of land C uptake was determined by the long-term trend in CUA and CUD as summarized in the figure 7 for the globe, NH and SH.

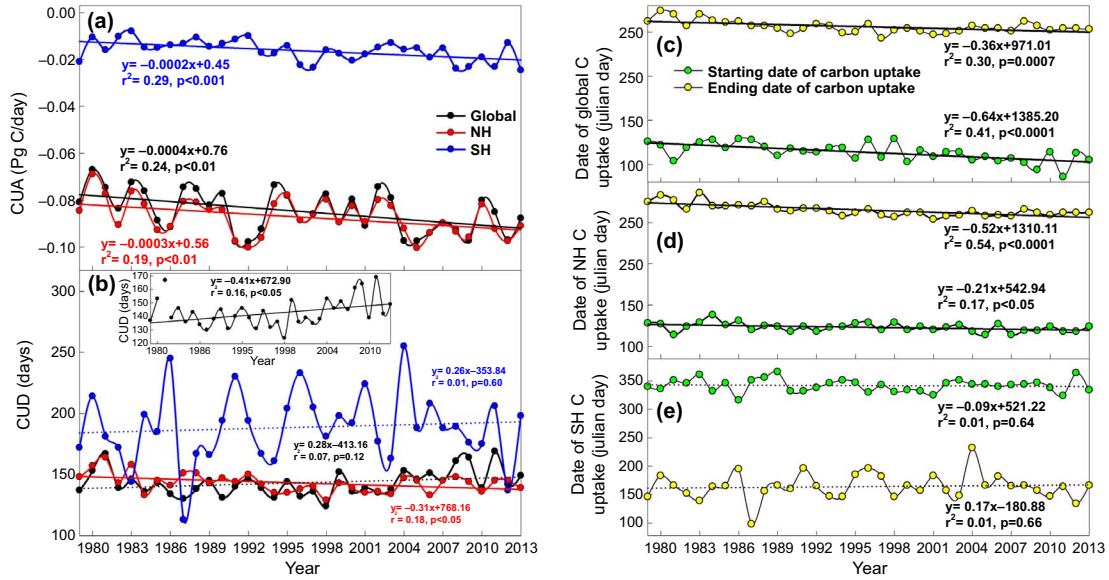

Figure 5. The long-term trend of CUA (*a*) and CUD (*b*) in the globe, NH and SH over 1979–2013. The insert is the long-term trend of CUD with exclusions of the extreme high value in 1981 in the globe. The long-term trend of starting and ending date of C uptake during 1979–2013 in the globe (*c*), NH (*d*) and SH (*e*). See figures 1 and 3 for the abbreviations.

The attribution process of CUA and CUD to the IAV of land C uptake

The IAV of global land C uptake significantly correlated with the IAV of CUA (r^2 = 0.42, $P < 0.0001$) and CUD ($r^2 = 0.22$, $P < 0.01$) (figures 6 (*a*) and (*b*)). Every 1 Pg C d^{-1} change in CUA resulted in a 76 Pg C changes in global land C uptake (figure 6(*a*)). A one-day change in global CUD leads to a global land C uptake change by 0.04 Pg C yr^{-1}, on average (figure 6(*b*)).

The IAV of land C uptake in the NH and SH were attributed to the IAV in CUA and CUD (figures 6 (*c*)–(*f*)). On average, C uptake changed 54 (figure 6 (*c*)) and 77 (figure 6(*e*)) Pg C yr^{-1} in the NH and SH respectively, with 1 Pg C change in CUA. A one-day change in CUD caused 0.05 (figure 6(*d*)) and 0.01 Pg C yr^{-1} (figure 6(*f*)) changes in annual C uptake in the NH and SH, respectively. The contributions of CUA and CUD to the IAV of land C uptake in the globe, NH, and SH are summarized in figure 7.

Discussion

Different roles of the NH, SH and ecosystems in contributing to the trend and IAV of land C uptake

The trends drivers of global land C uptake changes and IAV have different attributions in the NH and SH. NEE in the NH and SH both had large variability and a strong increasing trend of C uptake over the past 35 years. But the NH rather than the SH dominated the IAV of global NEE over recent decades, while both hemispheres contributed equivalently to the trend in C uptake.

Various ecosystems contributed differentially to the trend of C fluxes in the NH and SH. Tundra and arctic shrub lands and extra-tropical forests positively contributed most in the NH, which may be due to that climate change affects processes such as plant physiology, phenology, water availability, and vegetation dynamics, ultimately leading to increased plant productivity and vegetation cover at high northern latitudes in recent decades (Forkel *et al* 2016). The gradual replacement of herbaceous vegetation with shrubs and trees has been observed to increase C uptake at high northern latitudes (Forkel *et al* 2016, Liu *et al* 2015, Tucker *et al* 2001). Extra-tropical forest area increased and thus forest biomass has increased over the past decades (Food and Nations 2010, Pan *et al* 2011). Other ground-based studies showed that fire, logging, and other disturbances in boreal forest shifted the forest toward younger and early-successional forests, which contribute also to the increasing C sink (D'Arrigo *et al* 1987, Kasischke *et al* 2010). Results also demonstrate that grasslands and croplands positively contributed the trend of the NH land C sink. Cropland area didn't increase largely in the NH, but hybridization, irrigation and fertilization have increased crop production by threefold during the past five decades (Zeng *et al* 2014).

In the SH, semi-arid ecosystems were found to account for the largest fraction of the SH land sink trend. Semi-arid ecosystems in the SH have high sensitivity to precipitation and climate extremes (Yi *et al* 2015), which may absorb large amounts of C quickly at the suitable precipitation condition, positively contributing to the trend of C uptake (Ma *et al* 2016, Poulter *et al* 2014). For example, NEE in a forested savanna in Australia reached up to 2.5 tons C ha^{-1} when La Nina drove precipitation to 585 mm yr^{-1} (above a ∽300 mm yr^{-1} average) (Cleverly *et al* 2013). The predominance of semiarid ecosystems in explaining the SH land sink trend is consistent with widespread observations of woody

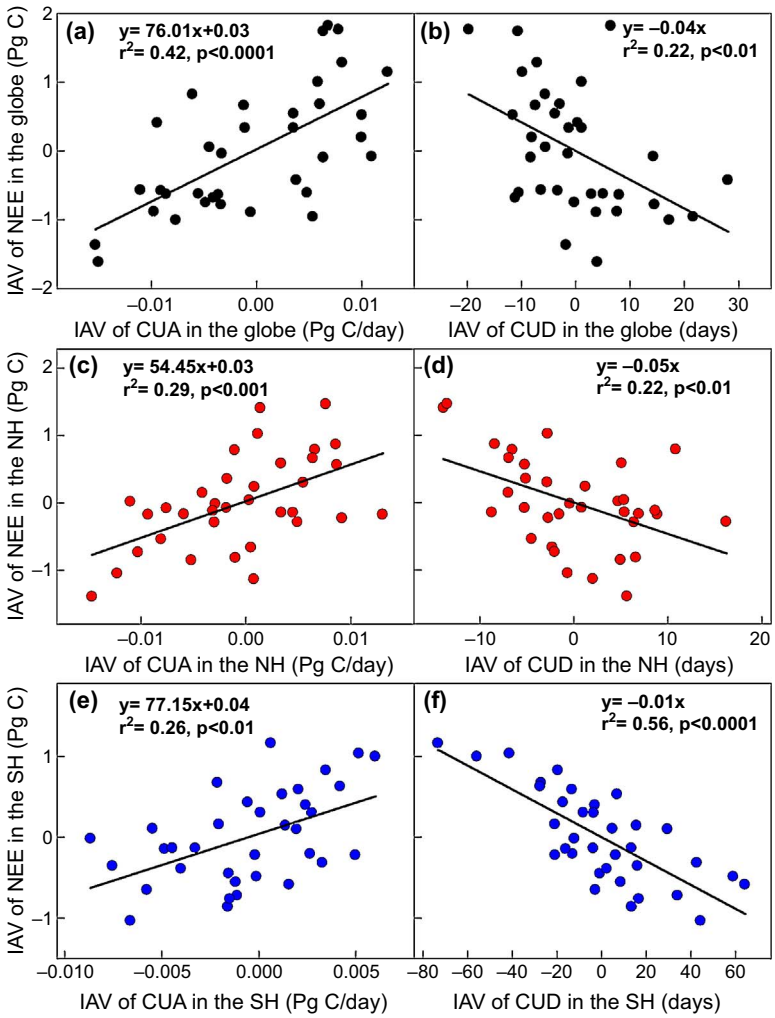

Figure 6. The relationships of the IAV in the land C uptake with the IAV of CUA and CUD across the globe (*a*), (*b*), the NH (*c*), (*d*), and the SH (*e*), (*f*) during 1979–2013. See figures 1 and 3 for abbreviations.

encroachment over semi-arid areas (Andela *et al* 2013) and increased vegetation greenness inferred from satellite remote sensing over recent decades (Andela *et al* 2013, Donohue *et al* 2009, Fensholt *et al* 2012).

For the IAV of C uptake, we found that semi-arid ecosystems played critical roles in both the NH and SH. It suggests that C uptake in the semi-arid ecosystems is highly dynamic from year to year. Our results are consistent with global analysis that showed that semi-arid ecosystems determine the IAV of global C uptake (Ahlström *et al* 2015). Besides the semi-arid ecosystems, grasslands and croplands also played an important role in the IAV of land C uptake in the NH. This may be due to that crop production is highly dependent on human activities, which vary largely across years. Changing growing times yearly such as single or double cropping, crop varieties such as high-yield but low-quality, low-yield but high-quality (Jain 2010, Zeng *et al* 2014), and cropland use patterns, like China's Grain for Green Project (Liu and Wu 2010), all will impact the production and change the year to year C uptake in the croplands and grasslands, whose contribution to the global IAV of C uptake deserve more study.

Attribution process understanding: regulations of CUA and CUD

This study decomposed annual NEE into CUA and CUD to better understand the attribution processes. We found that changes in ecosystem C uptake could be fundamentally explained by the changes in CUA and CUD (figure S2, figure 6), and the changes in CUD were determined by the starting and ending date of C uptake (figures 5(*c*)–(*e*)). In the NH, SH, and globe, CUA increased and enhanced land C uptake (figure 5 (*a*)). The other process, CUD, also lengthened across the globe and the SH, improving land C uptake even further. Advancing of starting date of C uptake was more than the advancing of ending date of C uptake, resulting in the extension of CUD in the globe (figure 5 (*c*)), but the SH CUD was attributable to the advancing of starting date of C uptake and postponing of ending date of C uptake (figure 5(*e*)). However, CUD decreased in the NH, with the advancing of starting date of C uptake contributing less than the advancing of ending date of C uptake. This partly offset the increased C sink by the increased CUA, making net C uptake trend same as that of the SH. For the C source process, our results also showed that C release amplitude (CRA) decreased

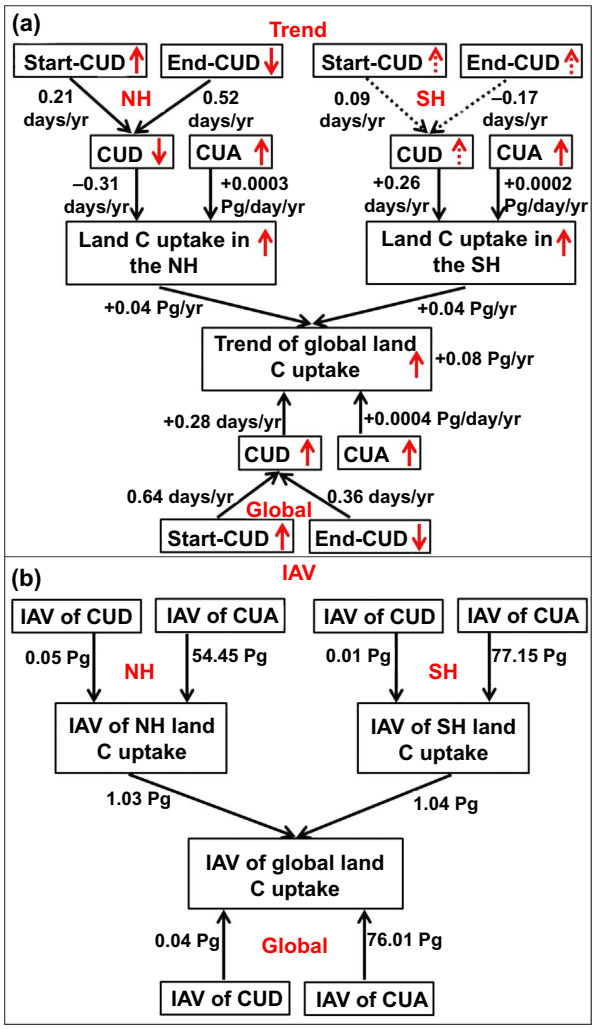

Figure 7. A conceptual framework for the regulations of CUA and CUD in the long term trend (*a*) and IAV (*b*) of land C uptake in the NH, SH, and globe for the period 1979–2013. Start-CUD: starting date of carbon uptake. End-CUD: ending date of carbon uptake. Solid lines indicate significant changes while dotted lines indicate non-significant changes. '+' indicates an increase while '−' indicates a decrease. '↑' means an increase in C uptake while '↓' means a decrease in C uptake. See figures 1 and 3 for abbreviations.

in the NH ($P < 0.05$), but had no significant changes in the globe and SH ($P > 0.05$) during 1979–2013, which partly contributed to the increasing net C uptake in the NH during the 35 year study period.

CUA, the peak of annual C uptake, means the maximal capacity of land C uptake. Long-term change in CUA largely impacts the long-term trend of C uptake. In the NH, increasing photosynthetic C uptake caused by climate change and mediated by changing vegetation cover (Forkel *et al* 2016), vegetation recovery (Kasischke *et al* 2010), afforestation (Food and Nations 2010, Pan *et al* 2011), and the agricultural green revolution (Gray *et al* 2014, Zeng *et al* 2014), may all contribute to improve the C uptake capacity during the peak growing seasons. For the SH, the semi-arid ecosystem in the SH have high sensitivity to the precipitation and climate extremes, which may absorb large amount of C quickly with the summer rainfall events, increasing the SH CUA (Cleverly *et al* 2013). Meanwhile, widespread observations of woody encroachment over semi-arid areas (Andela *et al* 2013) and increased vegetation greenness inferred from satellite remote sensing over recent decades (Andela *et al* 2013, Donohue *et al* 2009, Fensholt *et al* 2012) also increase photosynthetic C uptake and CUA in the SH as noted, but it is noteworthy that the SH CUA might be weakened by the increasing tropic forest deforestation (Pan *et al* 2011) and the increasing risks of drought and heat (Allen *et al* 2010, Phillips *et al* 2009, Zhao and Running 2010).

The increased CUD across the globe was mainly attributed to that the starting date of C uptake advanced more than the ending date. Richardson *et al* 2010 reported that climate warming stimulates photosynthesis more than respiration in the spring (Richardson *et al* 2010), leading to an earlier onset of carbon sink activity. Advanced beginning of spring and/or postponed ending of autumn seasons has been widely reported in the past studies on vegetation phenology (Linderholm 2006, Piao *et al* 2007, Smith *et al* 2004). However, in this study, we found that the ending date of ecosystem C uptake was advanced in the globe and NH over the past 35 years. The finding is supported by long-term observations at Barrow and

Mauna Loa, which shows the ending date of C uptake has advanced by 0.17 and 0.14 d yr^{-1}, respectively (Graven *et al* 2013). This is thought to be due to the autumn warming-induced increase in respiration being greater than that in photosynthesis, leading to an earlier end of the net C sink (Piao *et al* 2008).

Implications for seasonal changes in atmospheric CO_2

Our findings of the increased CUA and decreased CUD of C uptake in the NH provide explanations and insight into the seasonal amplitude and phase changes in atmospheric CO_2. The seasonal phase of atmospheric CO_2 concentration is quantified by the day of year with CO_2 concentration downward zero crossing, which corresponds to changes in the CUD in terrestrial ecosystem (Graven *et al* 2013, Piao *et al* 2008). The decreased CUD in the NH shortened the duration of atmospheric CO_2 decrease. The advanced starting and ending dates of land C uptake also led to the advance of starting and ending date of the atmospheric CO_2 decline, shifting its duration. This could explain the phenomenon that seasonal amplitude of atmospheric CO_2 in Hawaii was increased and accompanied by phase advances of about 7 days from mid-1970s to 1995 during the declining phase of the cycle (DeRosier *et al* 1996). The observed increasing seasonal amplitude of atmospheric CO_2 in the NH since 1960 could be also due to the increasing CUA (Graven *et al* 2013, Myneni *et al* 1997). So, the observed changes in CUA and CUD of land C uptake are crucial for better understand the dynamic changes of atmospheric CO_2 concentration.

In conclusion, we quantified the relative contributions of the NH, SH and different ecosystems to the trend and IAV of global land C uptake. We found that the IAV of the global land C sink during 1979–2013 was mostly attributed to the changes in the IAV of the land sink in the NH rather than the SH, but the trend of global land C uptake was attributed equally to both the NH and SH. For different ecosystem types, we found grasslands and croplands played an important role in the NH, while semi-arid ecosystems contributed substantially in the SH, for both the trend and IAV of C uptake. The trend and IAV of land C uptake can be fundamentally explained by the changes in CUA and CUD, but they worked in different ways in the NH and SH. The determinant role of C uptake capacity in the peak growing season and the starting and ending date of C uptake durations revealed in this study are crucial to better understand the mechanisms underlying the long-term trend and IAV of land C uptake and the consequent changes in atmospheric CO_2 dynamics.

Acknowledgments

We thank Dr Anders Ahlström for the map of land cover classes. This work was financially supported by the National Natural Science Foundation of China (31420103917, 31625006), the Ministry of Science and Technology of China (2013CB956300), and the 'Thousand Youth Talents Plan'. PCS acknowledges support from the U.S. National Science Foundation (1552976, 1632810). ZF gratefully acknowledges the China Scholarship Council for the financial support of a 24-month study at Montana State University.

References

Ahlbeck J R 2002 Comment on 'Variations in northern vegetation activity inferred from satellite data of vegetation index during 1981–1999' by L. Zhou *et al J. Geophys. Res. Atmos. 1984–2012* **107** ACH 9-1–ACH 9-2

Ahlström A *et al* 2015 The dominant role of semi-arid ecosystems in the trend and variability of the land CO_2 sink *Science* **348** 895–9

Allen C D *et al* 2010 A global overview of drought and heat-induced tree mortality reveals emerging climate change risks for forests *For. Ecol. Manage.* **259** 660–84

Andela N *et al* 2013 Global changes in dryland vegetation dynamics 1988–2008 assessed by satellite remote sensing: comparing a new passive microwave vegetation density record with reflective greenness data *Biogeosciences* **10** 6657–76

Ballantyne A *et al* 2012 Increase in observed net carbon dioxide uptake by land and oceans during the past 50 years *Nature* **488** 70–2

Chevallier F *et al* 2007 Contribution of the Orbiting Carbon Observatory to the estimation of CO_2 sources and sinks: theoretical study in a variational data assimilation framework *J. Geophys. Res. Atmos.* **112** D09307

Chevallier F *et al* 2010 CO_2 surface fluxes at grid point scale estimated from a global 21 year reanalysis of atmospheric measurements *J. Geophys. Res.* **115** D21307

Chevallier F *et al* 2005 Inferring CO_2 sources and sinks from satellite observations: Method and application to TOVS data *J. Geophys. Res. Atmos.* **110** D24309

Cleverly J *et al* 2013 Dynamics of component carbon fluxes in a semi-arid Acacia woodland, central Australia *J. Geophys. Res. Biogeosci.* **118** 1168–85

D'Arrigo R *et al* 1987 Boreal forests and atmosphere–biosphere exchange of carbon dioxide *Nature* **329** 321–3

DeRosier D *et al* 1996 Increased activity of northern vegetation inferred from atmospheric CO_2 measurements *Nature* **382** 11

Donohue R J *et al* 2009 Climate-related trends in Australian vegetation cover as inferred from satellite observations, 1981–2006 *Global Change Biol.* **15** 1025–39

Fang J *et al* 2001 Changes in forest biomass carbon storage in China between 1949 and 1998 *Science* **292** 2320–2

Fensholt R *et al* 2012 Greenness in semi-arid areas across the globe 1981–2007—an earth observing satellite based analysis of trends and drivers *Remote Sens. Environ.* **121** 144–58

Field C B *et al* 1998 Primary production of the biosphere: integrating terrestrial and oceanic components *Science* **281** 237–40

Food, Nations, A. O. o. t. U. 2010 *Global forest resources assessment 2010: Main report* Food and Agriculture Organization of the United Nations

Forkel M *et al* 2016 Enhanced seasonal CO_2 exchange caused by amplified plant productivity in northern ecosystems *Science* **351** 696–9

Frank D *et al* 2015 Effects of climate extremes on the terrestrial carbon cycle: concepts, processes and potential future impacts *Glob. Change Biol.* **21** 2861–80

Friedl M A *et al* 2010 MODIS Collection 5 global land cover: Algorithm refinements and characterization of new datasets *Remote Sens. Environ.* **114** 168–82

Graven H D *et al* 2013 Enhanced seasonal exchange of CO_2 by northern ecosystems since 1960 *Science* **341** 1085–9

Gray J M *et al* 2014 Direct human influence on atmospheric CO_2 seasonality from increased cropland productivity *Nature* **515** 398–401

Gu L *et al* 2009 Characterizing the seasonal dynamics of plant community photosynthesis across a range of vegetation types *Phenology of Ecosystem Processes* (Berlin: Springer) pp 35–58

Jain H 2010 *Green revolution: History, Impact and Future* (Houston, TX: Studium Press)

Kasischke E S *et al* 2010 Alaska's changing fire regime-implications for the vulnerability of its boreal forests *Can. J. For. Res.* **40** 1313–24

Keenan T F *et al* 2016 Recent pause in the growth rate of atmospheric CO_2 due to enhanced terrestrial carbon uptake *Nat. Commun.* **7** 13428

Kohlmaier G H *et al* 1989 Modelling the seasonal contribution of a CO_2 fertilization effect of the terrestrial vegetation to the amplitude increase in atmospheric CO_2 at Mauna Loa Observatory *Tellus B* **41** 487–510

Linderholm H W 2006 Growing season changes in the last century *Agric. For. Meteorol.* **137** 1–14

Liu C and Wu B 2010 *Grain for Green Programme in China: Policy making and implementation* (*Policy Briefing Series*) University of Nottingham, Nottingham (www.nottingham.ac.uk/cpi/documents/briefings/briefing-60-reforestation.pdf)

Liu Y Y *et al* 2015 Recent reversal in loss of global terrestrial biomass *Nat. Clim. Change* **5** 470–4

Ma X *et al* 2016 Drought rapidly diminishes the large net CO_2 uptake in 2011 over semi-arid Australia *Sci. Rep.* **6** 37747

Myneni R *et al* 1997 Increased Plant Growth in the Northern High Latitudes from 1981 to 1991 *Nature* **386** 698–702

Nemani R R *et al* 2003 Climate-driven increases in global terrestrial net primary production from 1982 to 1999 *Science* **300** 1560–3

Pan Y *et al* 2009 Separating effects of changes in atmospheric composition, climate and land-use on carbon sequestration of US Mid-Atlantic temperate forests *For. Ecol. Manage.* **259** 151–64

Pan Y *et al* 2011 A large and persistent carbon sink in the world's forests *Science* **333** 988–93

Phillips O L *et al* 2009 Drought sensitivity of the Amazon rainforest *Science* **323** 1344–7

Piao S *et al* 2008 Net carbon dioxide losses of northern ecosystems in response to autumn warming *Nature* **451** 49–52

Piao S *et al* 2007 Growing season extension and its impact on terrestrial carbon cycle in the Northern Hemisphere over the past 2 decades *Glob. Biogeochem. Cycles* **21** GB3018

Piao S *et al* 2006 Effect of climate and CO_2 changes on the greening of the Northern Hemisphere over the past two decades *Geophys. Res. Lett.* **33** L23402

Poulter B *et al* 2014 Contribution of semi-arid ecosystems to interannual variability of the global carbon cycle *Nature* **509** 600–3

Quéré C L *et al* 2013 The global carbon budget 1959–2011 *Earth System Science Data* **5** 165–85

Richardson A D *et al* 2010 Influence of spring and autumn phenological transitions on forest ecosystem productivity *Philos. Trans. R. Soc. B Biol. Sci.* **365** 3227–46

Schimel D S *et al* 2001 Recent patterns and mechanisms of carbon exchange by terrestrial ecosystems *Nature* **414** 169–72

Smith N V *et al* 2004 Trends in high northern latitude soil freeze and thaw cycles from 1988 to 2002 *J. Geophys. Res. Atmos. 1984–2012* **109** D12101

Tucker C J *et al* 2001 Higher northern latitude normalized difference vegetation index and growing season trends from 1982 to 1999 *Int. J. Biometeorol.* **45** 184–90

Wang X *et al* 2014 A two-fold increase of carbon cycle sensitivity to tropical temperature variations *Nature* **506** 212–5

Xia J *et al* 2015 Joint control of terrestrial gross primary productivity by plant phenology and physiology *Proc. Natl Acad. Sci.* **112** 2788–93

Yi C *et al* 2015 Focus on extreme events and the carbon cycle *Environ. Res. Lett.* **10** 070201

Yi C *et al* 2010 Climate control of terrestrial carbon exchange across biomes and continents *Environ. Res. Lett.* **5** 034007

Yi C *et al* 2014 Warming climate extends dryness-controlled areas of terrestrial carbon sequestration *Sci. Rep.* **4** 5472

Zeng N *et al* 2014 Agricultural Green Revolution as a driver of increasing atmospheric CO_2 seasonal amplitude *Nature* **515** 394–7

Zhao M and Running S W 2010 Drought-induced reduction in global terrestrial net primary production from 2000 through 2009 *Science* **329** 940–3

Zhou L *et al* 2001 Variations in northern vegetation activity inferred from satellite data of vegetation index during 1981 to 1999 *J. Geophys. Res. Atmos. 1984–2012* **106** 20069–83